A Comparison of Variational, Differential Quadrature and Approximate Closed Form Solution Methods for Buckling of Highly Flexurally Anisotropic Laminates

Zhangming Wu [1] and Gangadharan Raju [2], and Paul M Weaver [3],

ABSTRACT

The buckling response of symmetric laminates that possess strong flexural-twist coupling are studied using different methodologies. Such plates are difficult to analyse due to localised gradients in the mode shape. Initially, the energy method (Rayleigh-Ritz) using Legendre polynomials is employed and the difficulty of achieving reliable solutions for some extreme cases is discussed. To overcome the convergence problems, the concept of Lagrangian multiplier is introduced into the Rayleigh-Ritz formulation. The Lagrangian multiplier approach is able to provide the upper and lower bounds of critical buckling load results. In addition, mixed variational principles are used to gain a better understanding of the mechanics behind the strong flexural-twist anisotropy effect on buckling solutions. Specifically, the Hellinger-Reissner variational principle is used to study the effect of flexural-twist coupling on buckling and also to explore the potential

[1]Research Assistant, ACCIS, Dept. of Aerospace Engineering, Univ. of Bristol, Queen's Building, Bristol BS8 1TR, U.K.

[2]Research Assistant, ACCIS, Dept. of Aerospace Engineering, Univ. of Bristol, Queen's Building, Bristol BS8 1TR, U.K.

[3]Professor in Lightweight Structures, ACCIS, Dept. of Aerospace Engineering, Univ. of Bristol, Queen's Building, Bristol BS8 1TR, U.K. (corresponding author) E-mail: Paul.Weaver@bristol.ac.uk

for developing closed form solutions for these problems. Finally, solutions using the differential quadrature method are obtained. Numerical results of buckling coefficients for highly anisotropic plates with different boundary conditions are studied using the proposed approaches and compared with finite element results. The advantages of both Lagrangian multiplier theory and variational principle in evaluating buckling loads are discussed. In addition, a new simple closed form solution is shown for the case of a flexurally anisotropic plate with three sides simply supported and one long edge free.

Keywords: Buckling, Flexural-twist coupling, Lagrangian Multiplier, Hellinger-Reissner variational principle, Differential Quadrature Method

INTRODUCTION

Laminated composite structures provide structural engineers with extended design space and tailorability options which helps facilitate the design of efficient, lightweight structures. Most laminated structures are designed to be balanced and symmetric with angle plies such that the coupling between in-plane extension, contraction with shear is avoided and any combination of these with bending or twisting is also avoided yet still exhibit flexural-twist coupling to various degrees. But, in the case of highly anisotropic composite plates, the effect of flexural-twist coupling may be significant in the numerical evaluation of critical buckling load. Therefore, a numerical methodology has to be developed for buckling analysis of highly anisotropic composite structures. Earlier works of buckling analysis on anisotropic plates were reported on the study of plywood plates (Balabuch 1937; Thielemann 1950; Green and Hearmon 1945). Green and Hearmon (Green and Hearmon 1945) derived the formulation for buckling analysis of anisotropic plates using Fourier series expansions, and also explored approximate closed-form solutions of buckling load for infinite long anisotropic plate. Ashton and Waddoups (Ashton and Waddoups 1969; Ashton 1969) applied the Rayleigh-Ritz

(RR) method to perform stability and dynamics analysis of anisotropic plates with various boundary conditions. Later, Whitney (Whitney 1972) employed the Fourier series approach proposed by Green to solve the vibration problem of anisotropic plates with clamped edges. Chamis (Chamis 1969) used Galerkin's method to perform the buckling analysis of anisotropic plates and concluded that neglecting flexural-twist anisotropy could lead to non conservative buckling loads.

Nemeth (Nemeth 1986) defined the nondimensional parameters associated with flexural-twist anisotropy and analysed the effects of flexural-twist anisotropy on buckling of symmetric laminates. Tang *et al.* (Tang and Sridharan 1990) and Grenestedt (Grenestedt 1989) employed a pertubation technique to study the effect of flexural-twist anisotropy on buckling strength. Weaver (Weaver 2006) developed approximate closed-form (CF) expressions to study the effect of flexural-twist anisotropy on buckling load of long anisotropic plates with simply-supported sides subject to compression. Weaver and Nemeth(Weaver and Nemeth 2007) derived the bounds for non dimensional parameters governing the buckling of anisotropic plates and this study provided insight into composite tailoring for improving buckling resistance. Herencia *et al.*(Herencia et al. 2010) obtained closed from solutions for buckling of long plates with flexural-twist anisotropy with the short edges simply supported and with the longitudinal edges simply supported, clamped, or elastically restrained in rotation under axial compression. All of the above approaches give accurate results when applied to plates with low to moderate flexural-twist anisotropy under different boundary conditions. However, when applied to laminates with extremely highly flexural-twist anisotropy, they suffer from the issues of either very slow convergence or inaccurate results.

Initially, the RR method was applied to study the above problem using different orthogonal polynomials as admissible functions of plate deflection. Many works have been reported in literature (Bhat 1985; Smith et al. 1999; Pandey and Sherbourne 1991; Liew and Wang 1995; Chow et al. 1992) using orthogonal polynomials in RR method for structural analysis. The results obtained using orthogonal polynomials show better convergence when compared to Fourier series or beam mode shape functions. The reason is that, non-periodic polynomial functions are better equipped than periodic trigonometric functions to capture localised features, such as strong gradients in the buckling mode shape. In the present work, Legendre polynomials were chosen as test functions to solve the composite plate buckling problem and study the effect of bending-twisting coupling coefficients(D_{16} and D_{26}) on buckling solutions(Nemeth 1986). The method was not able to capture accurate buckling load results for some extreme cases, such as the $[+45]_n$ all simply supported laminates and the $[+30]_n$ one edge free laminates. The reason can be attributed to the non-satisfaction of natural boundary conditions term by term which results in the slow convergence of the RR method. In addition, the decreased accuracy of differentiation on the obtained approximate deflection function will cause further errors in evaluation of moments and forces.

In order to overcome convergence problems and improve the buckling results, methodologies based on Lagrangian multipliers, Hellinger-Reissner (H-R) variational principle (Reissner 1950) and differential quadrature method (DQM) (Bellman 1971) are considered in this work. Following Budiansky and Hu's approach (Budiansky and Hu 1946), the Lagrangian multiplier method using Legendre polynomials is extended to study our test problems. The upper and lower bounds of the solution can be obtained by varying the number of Lagrangian multiplier terms and this concept is used for the evaluation of buckling load. In the approach based on the H-R principle, the deflection and moments are allowed to vary independently(Plass et al. 1962), while the relation between moments and deflection (curvature) are weakly constrained in the defined functional. The constraints in the functional between the different variables (functions) can be considered as the method of Lagrangian multipliers(Chien 1984). In the current work, the deflection and moments are represented independently using Legendre polynomials and the chosen polynomials satisfy the boundary conditions in terms of deflection (w) and moments (M_x, M_y, M_{xy}). This approach is then applied to our test problems and the convergence of the buckling load results is studied. Furthermore, as an alternative methodology to energy methods, DQM is also employed. DQM is based on the quadrature method to approximate the derivatives of a function and can be applied directly to solve the differential equation with appropriate boundary conditions. Sherbourne *et al* (Sherbourne and Pandey 1991) studied the accuracy and convergence of DQM for buckling analysis of anisotropic composite plates under linearly varying compression load. Darvizeh *et al* (Darvizeh et al. 2004) compared the performance of DQM with the RR method for buckling analysis of composite plates. Herein, the buckling analysis of highly anisotropic laminates is studied using DQM and the accuracy of the results are compared with the other proposed approaches.

Thus the motivation of the present work is: (i) to develop robust and generalized methodologies for the buckling analysis of symmetric laminates with strong flexural-twisting coupling, (ii) to study the effects of flexural-twist anisotropy on buckling of long and short flexurally anisotropic plates under two sets of boundary conditions using the proposed approaches and validate the results using finite element method. Finally, a new approximate closed form solution is also offered to provide a lower bound estimate for the buckling load of a long, flexurally anisotropic plate with three sides simply supported and one long side free.

FLEXURALLY ANISOTROPIC PLATE

Flexurally anisotropic plate formulation

For a symmetrically laminated anisotropic plate subjected to uniaxial compression loading, the plate buckling behavior is governed by

$$\begin{aligned} D_{11}\frac{\partial^4 w}{\partial x^4} + 2(D_{12}+2D_{66})\frac{\partial^4 w}{\partial x^2 \partial y^2} + D_{22}\frac{\partial^4 w}{\partial y^4} \\ + 4D_{16}\frac{\partial^4 w}{\partial x^3 \partial y} + 4D_{26}\frac{\partial^4 w}{\partial x \partial y^3} = N_x \frac{\partial^2 w}{\partial x^2} \end{aligned} \tag{1}$$

where $D_{ij}(i,j = 1,2,6)$ and w are bending stiffness and out-of-plane deflection function of plate, respectively. The following four non-dimensional parameters of bending stiffness developed by Nemeth(Nemeth 1986),

$$\alpha = \sqrt[4]{\frac{D_{11}}{D_{22}}};\ \beta = \frac{(D_{12}+2D_{66})}{\sqrt{D_{11}D_{22}}};\ \gamma = \frac{D_{16}}{\sqrt[4]{D_{11}^3 D_{22}}};\ \delta = \frac{D_{26}}{\sqrt[4]{D_{22}^3 D_{11}}} \tag{2}$$

reflect the effects of orthotropy (α, β) and flexural-twist anisotropy (γ, δ) on plate buckling response. The bounds of these parameters were found to be $\alpha > 0$, $-1 < \beta < 3$, $|\gamma, \delta| < 1$ (Weaver and Nemeth 2007). When the absolute values of γ or δ are large, the plate is highly anisotropic and it may cause difficulties in the evaluation of its buckling load. In this paper, anisotropic plates with two different boundary conditions (Fig. 1) are considered, all simply-supported (SSSS) and one free edge and others simply-supported (SSSF).

RAYLEIGH-RITZ FORMULATION

The total potential energy of a plate under uniaxial compression is expressed as (Ashton and Waddoups 1969)

$$\Pi = U_b + \lambda U_T = \text{stationary value} \tag{3}$$

where U_b is the strain energy of plate, U_T is potential energy due to in-plane loads and λ is the unknown buckling load proportionality factor. The potential energy can be expressed in the following convenient form with respect to normalised coordinates,

$$\tilde{U}_b = \int_{-1}^{1}\int_{-1}^{1}\left[D_{11}\left(\frac{\partial^2 w}{\partial \xi^2}\right)^2 + 2\rho^2 D_{12}\frac{\partial^2 w}{\partial \xi^2}\frac{\partial^2 w}{\partial \eta^2} + \rho^4 D_{22}\left(\frac{\partial^2 w}{\partial \eta^2}\right)^2 \right.$$
$$\left. + 4\rho^2 D_{66}\left(\frac{\partial^2 w}{\partial \xi \partial \eta}\right)^2 + 2\rho D_{16}\frac{\partial^2 w}{\partial \xi^2}\frac{\partial^2 w}{\partial \xi \partial \eta} + 2\rho^3 D_{26}\frac{\partial^2 w}{\partial \eta^2}\frac{\partial^2 w}{\partial \xi \partial \eta}\right] d\xi d\eta \quad (4)$$

$$\tilde{U}_T = \int_{-1}^{1}\int_{-1}^{1} N_x \left(\frac{\partial w}{\partial \xi}\right)^2 d\xi d\eta \quad (5)$$

where $\rho = a/b$ is the aspect ratio and a, b are the length and width of the plate, respectively. The nondimensional parameters ξ, η are defined as $\xi = 2x/a$, $\eta = 2y/b$ ($\xi, \eta \in [-1, 1]$). The out-of-plane deflection of plate is assumed to be of the form,

$$w(\xi, \eta) = \sum_{m=1}^{M}\sum_{n=1}^{N} A_{mn} X_m(\xi) Y_n(\eta) \quad (6)$$

where A_{mn} are the unknown deflection coefficients, $X_m(x)$ and $Y_n(y)$ are admissible functions satisfying the geometry boundary conditions. The numbers M and N denote the number of admissible functions $X_m(x)$ and $Y_n(y)$ employed in RR method, respectively. In this work Legendre polynomials are chosen for analysis due to superior convergence properties in capturing localised features, defined as,

$$P_1 = 1,\ P_2 = \xi,\ P_3 = \frac{1}{2}(3\xi^2 - 1)\ \cdots$$
$$P_{i+1}(\xi) = \sum_{j=0}^{J}(-1)^j \frac{(2i-2j)!}{2^i j!(i-j)!(i-2j)!}\xi^{i-2j} \quad (7)$$
$$j = \frac{i}{2}(i = 0, 2, 4, \cdots),\ \ \frac{i-1}{2}(i = 1, 3, 5, \cdots)$$

The admissible functions when applied to the above mentioned plate boundary conditions can be written in the following form,

$$\begin{aligned} X_m(\xi) &= (1-\xi)^{\iota}(1+\xi)^{\iota}P_m(\xi) \\ Y_n(\eta) &= (1-\eta)^{\iota}(1+\eta)^{\iota}P_n(\eta) \end{aligned} \tag{8}$$

where $\iota = 0, 1, 2$ for the boundary conditions of free, simply-supported and clamped edges, respectively. The total potential energy Π is then minimised with respect to A_{mn} and the resulting matrix expression is given as,

$$\{\mathbf{K} + \lambda\mathbf{L}\}\{\mathbf{A}\} = 0 \tag{9}$$

where $[\mathbf{A}] = [A_{11}, A_{12} \cdots, A_{MN}]^T$. The elements of matrix $\mathbf{K}$ and $\mathbf{L}$ are given as follows,

$$
\begin{aligned}
&K_{ij} = U_{b,mnrs} = \\
&\int_{-1}^{1}\int_{-1}^{1}\Big[D_{11}X_{m,\xi\xi}Y_nX_{r,\xi\xi}Y_s \\
&+\rho^2 D_{12}(X_mY_{n,\eta\eta}X_{r,\xi\xi}Y_s + X_{m,\xi\xi}Y_nX_rY_{s,\eta\eta}) \\
&+\rho^4 D_{22}X_{m,\xi\xi}Y_nX_{r,\xi\xi}Y_s + \rho^2 D_{66}X_{m,\xi}Y_{n,\eta}X_{r,\xi}Y_{s,\eta} \\
&+\rho D_{16}(X_{m,\xi}Y_{n,\eta}X_rY_{s,\eta\eta} + X_mY_{n,\eta\eta}X_{r,\xi}Y_{s,\eta\eta}) \\
&+\rho^3 D_{26}(X_{m,\xi\xi}Y_nX_{r,\xi}Y_{s,\eta} + X_{m,\xi}Y_{n,\eta}X_{r,\xi\xi}Y_s)\Big]d\xi d\eta \\
&L_{ij} = U_{T,mnrs} = \frac{a^2}{4}\int_{-1}^{1}\int_{-1}^{1}X_{m,\xi}Y_nX_{r,\xi}Y_s d\xi d\eta \\
&m,r = 1,2,\cdots,M, \quad n,s = 1,2,\cdots,N \\
&i = l(r-1)+s, \quad j = l(m-1)+n, \\
&l = 1,2,\cdots,M; \;\; i,j = 1,2,\cdots,M\times N
\end{aligned}
\tag{10}
$$

The eigenvalue problem is then solved for λ and the critical buckling load (N_x^{cr}) is given by the lowest non-zero eigenvalue (λ_{cr}) of Eq. (9). The nondimensional buckling coefficient is defined by,

$$
K_x^{cr} = \frac{N_x^{cr}b^2}{\pi^2\sqrt{D_{11}D_{22}}} \tag{11}
$$

The RR method applied to anisotropic plates with low flexural-twist anisotropy converged to an accurate buckling load results with few Legendre polynomials. But, for plates with high flexural twist anisotropy, the convergence of the RR method became very slow due to the difficulty associated in satisfying the natural boundary conditions along the edges of the plate and the highly localised deformations near the boundaries. Also, the numerical ill-conditioning problem associated with use of more terms to get satisfactory results limits the practical benefits of the RR method. Therefore, new methodologies have to be developed to overcome the convergence problems of the RR method which are explained in the subsequent sections.

THE LAGRANGIAN MULTIPLIER METHOD

The methodology using Lagrangian multipliers (LM) based on Budiansky's approach (Budiansky and Hu 1946) was extended to study the effect of flexural-twist anisotropy on buckling load solutions. In the RR method, the coefficient terms of Legendre polynomials in Eq.(8) under different boundary conditions are functions of nondimensional coordinates which makes the admissible functions of Eq. (6) non-orthogonal and, therefore, less efficient. In this approach, the admissible functions, expanded as a series are forced to satisfy the essential boundary conditions using Lagrangian multipliers rather than term by term satisfaction of boundary conditions, as in the RR method. This approach results in both orthogonality of admissible functions and satisfaction of essential boundary conditions. In this work, the admissible functions of Eq. (6) are expanded using Legendre polynomials directly, $X_m = P_m(\xi), Y_n = P_n(\eta)$ and the functional of Eq. (3) becomes,

$$\Pi_{LM} = U_b + \lambda U_T + \sum_{p,q} \Lambda \cdot H(A_{mn}) \tag{12}$$

where Λ is a Lagrangian Multiplier and $H(A_{mn})$ is a function of undetermined coefficients (A_{mn}), which are related to the boundary conditions. The terms p, q denote the number of Lagrangian Multipliers used for the constrained edges. The geometric boundary conditions along the edges are discretized independently using admissible functions and they are forced to be satisfied using Lagrangian multipliers. For example, the boundary condition ($w = 0$ at $\xi = 1$) for a simply-supported edge are

$$
\begin{aligned}
&\sum_{m}^{M}\sum_{n}^{N} A_{mn}X_m(1)Y_n(\eta) = 0 \Rightarrow \\
&\sum_{m}^{M} A_{m1}X_m(1)Y_1(\eta) = 0, \ \ \sum_{m}^{M} A_{m2}X_m(1)Y_2(\eta) = 0, \cdots \\
&\sum_{m}^{M} A_{mp}X_m(1)Y_p(\eta) = 0, \ \cdots \\
&\Rightarrow \sum_{p}^{P} \Lambda_p \sum_{m}^{M} A_{mp}X_m(1) = 0 \ \ (p = 1, 2, \cdots P \leq N)
\end{aligned}
\tag{13}
$$

For a SSSS plate, the last term in Eq. (12) is expressed as,

$$
\begin{aligned}
&\sum_{p,q} \Lambda H(A_{mn}) = \\
&\sum_{p_1}^{P} \Lambda_{p_1} \sum_{m}^{M} A_{mp_1} + \sum_{p_2}^{P} \Lambda_{p_2} \sum_{m}^{M} A_{mp_2}(-1)^{m+1} \\
&+ \sum_{q_1}^{Q} \Lambda_{q_1} \sum_{n}^{N} A_{q_1 n} + \sum_{q_2}^{Q} \Lambda_{q_2} \sum_{n}^{N} A_{q_2 n}(-1)^{n+1} \\
&(P < N; Q < M)
\end{aligned}
\tag{14}
$$

where p_1, p_2, q_1, q_2 denote the number of Lagrangian Multipliers that are used to constrain the deflection boundary conditions along the edges of $\xi = 1, \xi = -1, \eta = 1, \eta = -1$, respectively.

Other boundary conditions are captured in a similar way. After the minimizing process, the following matrix expression is obtained,

$$
\left\{ \begin{bmatrix} \mathbf{K} & \mathbf{H} \\ \mathbf{H}^T & \mathbf{O} \end{bmatrix} + \lambda \begin{bmatrix} \mathbf{L} & \mathbf{O} \\ \mathbf{O} & \mathbf{O} \end{bmatrix} \right\} \left\{ \begin{array}{c} \mathbf{A} \\ \boldsymbol{\Lambda} \end{array} \right\} = 0 \tag{15}
$$

where matrix $[\mathbf{O}]$ is the null matrix and $[\mathbf{A}]$, $[\mathbf{K}]$, $[\mathbf{L}]$ are defined in Eq. (9)

and (10). $[\boldsymbol{\Lambda}]$ is the set of Lagrange Multipliers. The term λ is the eigenvalue of buckling load. Dimensions of the matrices $[\mathbf{K}]$, $[\mathbf{H}]$, $[\mathbf{L}]$ are $MN \times MN$, $MN \times 2(P+Q)$, $MN \times MN$ respectively.

Elements in matrix $\mathbf{H}$ are given as follows, in which the row index (i) is defined in Eq. (10) and the column index $j = l(p_1 + p_2) + (q_1 + q_2)$.

$$H_{ij}(j \leq 2P) = \begin{cases} (-1)^{r+1} & j = 2s - 1 \\ 1 & j = 2s \\ 0 & \text{others} \end{cases} \tag{16}$$

$$H_{ij}(j > 2P) = \begin{cases} (-1)^{s+1} & j = 2r - 1 \\ 1 & j = 2r \\ 0 & \text{others} \end{cases} \tag{17}$$

The number of Lagrangian multipliers along each edge (P or Q) is required to be less than the number of terms of admissible functions (M or N). By altering the values of P and Q, the upper and lower bounds of critical buckling load (N_x^{cr}) are obtained. The merits of using Lagrangian multipliers are: (i) improvements in the convergence of the RR method. (ii) identification of upper and lower bounds of the critical buckling loads. Another way to address the convergence problem of buckling of composite plates with high flexural-twist anisotropy is to rely on generalised variational principles such as that explained in the next section(Washizu 1975).

HELLINGER-REISSNER VARIATIONAL PRINCIPLE

The slow convergence of the RR method on anisotropic plates, discussed in the RR formulation section, is mainly due to none satisfaction of natural (force) boundary conditions and the highly localised deformation in the vicinity of boundaries. We now use the variational form, given by Hellinger and Reissner (Reissner

1950), to solve the buckling problem of anisotropic plates. The H-R principle, in terms of out-of-plane deflection and bending moments, is given by

$$\begin{aligned}\Pi_{HR} = \iint_S \Bigg\{ & \left(-M_x \frac{\partial^2 w}{\partial x^2} - M_y \frac{\partial^2 w}{\partial y^2} - M_{xy} \frac{\partial^2 w}{\partial x \partial y} \right) \\ & - \frac{1}{2}(d_{11} M_x^2 + d_{22} M_y^2 + 2d_{12} M_x M_y + 2d_{16} M_x M_{xy} \\ & + 2d_{26} M_y M_{xy} + d_{66} M_{xy}^2) \Bigg\} dxdy\end{aligned} \tag{18}$$

where $d_{ij}(i, j = 1, 2, 6)$ is the bending compliance (D^{-1}) defined as,

$$\begin{bmatrix} d_{11} & d_{12} & d_{16} \\ d_{12} & d_{22} & d_{26} \\ d_{16} & d_{26} & d_{66} \end{bmatrix} = \begin{bmatrix} D_{11} & D_{12} & D_{16} \\ D_{12} & D_{22} & D_{26} \\ D_{16} & D_{26} & D_{66} \end{bmatrix}^{-1} \tag{19}$$

The bending moments M_x, M_y, M_{xy} are allowed to vary independently in Eq. (18) and expanded in nondimensional form by the following expression,

$$\begin{aligned} M_x \rightarrow M_\xi(\xi, \eta) &= \sum_{m=1}^{M_1} \sum_{n=1}^{N_1} \phi_{mn}^{(a)} X_m^{(a)}(\xi) Y_n^{(a)}(\eta) \\ M_y \rightarrow M_\eta(\xi, \eta) &= \sum_{m=1}^{M_2} \sum_{n=1}^{N_2} \phi_{mn}^{(b)} X_m^{(b)}(\xi) Y_n^{(b)}(\eta) \\ M_{xy} \rightarrow M_{\xi\eta}(\xi, \eta) &= \sum_{m=1}^{M_3} \sum_{n=1}^{N_3} \phi_{mn}^{(c)} X_m^{(c)}(\xi) Y_n^{(c)}(\eta) \end{aligned} \tag{20}$$

where $M_1, N_1, ..., N_3$ denote the total number used for each admissible function $X_m^{(a)}, Y_n^{(a)}, ..., Y_n^{(c)}$ of the bending moments, respectively. Substituting Eq. (6) and (20) into Eq. (18) and performing the usual minimizing procedure, a set of algebraic equations in matrix form is given as

$$\left\{ \begin{bmatrix} \mathbf{O} & \mathbf{B} \\ \mathbf{B}^T & \mathbf{C} \end{bmatrix} + \lambda \begin{bmatrix} \mathbf{L} & \mathbf{O} \\ \mathbf{O} & \mathbf{O} \end{bmatrix} \right\} \left\{ \begin{array}{c} \mathbf{A} \\ \Phi \end{array} \right\} = 0 \tag{21}$$

where $[\mathbf{L}]$ is defined in Eq. (10). Matrix $[\mathbf{A}]$ and $[\Phi] = [\phi_{11}^{(a)}, \phi_{12}^{(a)}, \cdots, \phi_{M_1N_1}^{(a)}, \phi_{11}^{(b)}, \phi_{12}^{(b)}, \cdots, \phi_{M_2N_2}^{(b)}, \phi_{11}^{(c)}, \phi_{12}^{(c)}, \cdots, \phi_{M_3N_3}^{(c)}]^T$ are the undetermined coefficients of deflection and moments, respectively. Again, λ is the eigenvalue of buckling load as defined in Eq. (3) and (15). Dimensions of the matrices $[\mathbf{B}]$ and $[\mathbf{C}]$ are $MN \times (M_1N_1 + M_2N_2 + M_3N_3)$, $(M_1N_1 + M_2N_2 + M_3N_3) \times (M_1N_1 + M_2N_2 + M_3N_3)$ respectively.

Matrix $[B]$ contains three submatrices, $[B] = [B_{11} \quad B_{12} \quad B_{13}]$ and are given by,

$$\begin{aligned} B_{11,mnrs} &= \int_{-1}^{1} \int_{-1}^{1} X_{m,\xi\xi} Y_n X_r^{(a)} Y_s^{(a)} d\xi d\eta \\ B_{12,mnrs} &= \int_{-1}^{1} \int_{-1}^{1} X_m Y_{n,\eta\eta} X_r^{(b)} Y_s^{(b)} d\xi d\eta \\ B_{13,mnrs} &= \int_{-1}^{1} \int_{-1}^{1} X_{m,\xi} Y_{n,\eta} X_r^{(c)} Y_s^{(c)} d\xi d\eta \end{aligned} \tag{22}$$

Matrix $[C]$ contains nine submatrices which are defined using,

$$[\mathbf{C}] = \begin{bmatrix} C_{11} & C_{12} & C_{13} \\ C_{12}^T & C_{22} & C_{23} \\ C_{13}^T & C_{23}^T & C_{33} \end{bmatrix} \tag{23}$$

$$
\begin{aligned}
C_{11,mnrs} &= \int_{-1}^{1}\int_{-1}^{1} X_m^{(a)}Y_n^{(a)}X_r^{(a)}Y_s^{(a)}d\xi d\eta \\
C_{12,mnrs} &= \int_{-1}^{1}\int_{-1}^{1} X_m^{(a)}Y_n^{(a)}X_r^{(b)}Y_s^{(b)}d\xi d\eta \\
C_{13,mnrs} &= \int_{-1}^{1}\int_{-1}^{1} X_m^{(a)}Y_n^{(a)}X_r^{(c)}Y_s^{(c)}d\xi d\eta \\
C_{22,mnrs} &= \int_{-1}^{1}\int_{-1}^{1} X_m^{(b)}Y_n^{(b)}X_r^{(b)}Y_s^{(b)}d\xi d\eta \\
C_{23,mnrs} &= \int_{-1}^{1}\int_{-1}^{1} X_m^{(b)}Y_n^{(b)}X_r^{(c)}Y_s^{(c)}d\xi d\eta \\
C_{33,mnrs} &= \int_{-1}^{1}\int_{-1}^{1} X_m^{(c)}Y_n^{(c)}X_r^{(c)}Y_s^{(c)}d\xi d\eta
\end{aligned}
\tag{24}
$$

Finally, separate expressions for the deflection function (w) and bending moments (M_x, M_y, M_{xy}) are applied to Eqs. (18)-(24), such that both the deflection and moment boundary conditions are satisfied. For example, using Legendre polynomials, the moment functions for the SS or free edges are assumed to be,

$$
\begin{aligned}
M_\xi(\xi,\eta) &= \sum_{m=1}\sum_{n=1}\phi_{mn}^{(a)}(1-\xi^2)P_m(\xi)P_n(\eta) \\
M_\eta(\xi,\eta) &= \sum_{m=1}\sum_{n=1}\phi_{mn}^{(b)}P_m(\xi)(1-\eta^2)P_n(\eta) \\
M_{\xi\eta}(\xi,\eta) &= \sum_{m=1}\sum_{n=1}\phi_{mn}^{(c)}P_m(\xi)P_n(\eta)
\end{aligned}
\tag{25}
$$

The advantage of this approach is that both essential and natural boundary conditions can be both modelled and satisfied independently and this helps in improving the convergence of buckling problems.

DIFFERENTIAL QUADRATURE METHOD

The differential quadrature method (DQM) was introduced by Bellman and Casti (Bellman 1971) to solve initial and boundary value problems. In DQM, the derivative of a function, with respect to a space variable at a given discrete grid point, is approximated as a weighted linear sum of the function values at all of the grid points in the entire domain of that variable. The n^{th} order partial derivative of a function *f(x)* at the i^{th} discrete point is approximated by

$$\frac{\partial^n f(x_i)}{\partial x^n} = A_{ij}^{(n)} f(x_j) \quad i = 1, 2, ..., N \tag{26}$$

where x_i= set of discrete points in the x direction; and $A_{ij}^{(n)}$ is the weighting coefficients of the n^{th} derivative and repeated index j indicates summation from 1 to N. The choice of the grid distribution for computation of weighting coefficient matrices and methods to model multiple boundary conditions are discussed by Shu (Shu 2000). DQM is fast and computationally less expensive to achieve results with similar levels of accuracy as variational methods. In this work, the non uniform grid distribution given by the Chebyshev-Gauss-Labotto points are used for the computation of weighting matrices and is given by

$$X_i = \frac{1}{2}[1 - cos(\frac{i-1}{N-1}\pi)] \quad i = 1, 2, ...n \tag{27}$$

where n is the number of grid points. The DQM representation of Eq. (1) is given by

$$\begin{aligned} &D_{11}\sum_{k=1}^{n_x} A_{ik}^{(4)} w_{kj} + 2(D_{12} + 2D_{66})\sum_{k=1}^{n_x}\sum_{m=1}^{n_y} A_{ik}^{(2)} B_{jm}^{(2)} w_{km} + D_{22}\sum_{m=1}^{n_y} B_{jm}^{(4)} w_{im} \\ &+4D_{16}\sum_{k=1}^{n_x}\sum_{m=1}^{n_y} A_{ik}^{(3)} B_{jm}^{(1)} w_{km} + 4D_{26}\sum_{k=1}^{n_x}\sum_{m=1}^{n_y} A_{ik}^{(1)} B_{jm}^{(3)} w_{km} = \bar{N}_x \sum_{k=1}^{n_x} A_{ik}^{(2)} w_{kj} \end{aligned} \tag{28}$$

$$i = 1, ..., n_x; \quad j = 1, ..., n_y$$

where $A_{ik}^{(n)}, B_{jm}^{(n)}$ represent the contributions of the n^{th} order partial derivatives with respect to x and y directions, respectively. The boundary conditions can be written in DQM form analogously. Eq. (28) shows that DQM reduces the governing differential equation into a set of algebraic equations and provides an attractive procedure for solving the buckling problem. In this work, DQM was applied to study the buckling of laminated plates with strong flexural-twist anisotropy and the accuracy of the results was investigated.

NUMERICAL RESULTS AND DISCUSSION

Highly flexurally anisotropic plate

In this work, symmetrical laminates made from P100/AS3501 prepreg material, which has potentially high levels of anisotropy in laminated structures, (Weaver 2006) was studied under different boundary conditions. The material properties of P100/AS3501 are E_{11}=369GPa, E_{22}=5.03GPa, G_{12}=5.24GPa and ν_{12}=0.31. The proposed approaches were applied to obtain the buckling solutions of flexurally anisotropic plates with unidirectional layups ($[+\theta]_n$). Bounds of the nondimensional parameters associated with flexural-twist anisotropy for the P100/AS3501 material are: $0 < |\gamma, \delta| < 0.92$ for $[+\theta]_n$ layups (Weaver and Nemeth 2007). Finite Element (FE) analysis was carried out using ABAQUS for validation of the proposed approaches. An 8-noded shell element with reduced integration (S8R5) was chosen to discretise the plate for buckling analysis and mesh density is chosen to be 100×5 to get accurate results. Results were also validated with respect those previously obtained (Weaver 2006; Herencia et al. 2010).

SSSS long plate

The buckling analysis of anisotropic long plates ($a/b = 5$) with SSSS boundary conditions was carried out using RR and DQ methods. The buckling loads converge to a constant value (within 5%) for aspect ratios of plates of $a/b >$

$3\sqrt[4]{D_{11}/D_{22}}$ (Weaver 2006). Weaver (Weaver 2006) derived two CF expressions for obtaining approximate solutions to the buckling coefficients of the SSSS anisotropic long plate and also developed an iterative method to compute what was shown to be, within a small margin, an exact value. Later, Herencia *et al* (Herencia et al. 2010) derived another CF expression for this case and achieved better approximate closed form solutions. The buckling results obtained by the RR method with Legendre polynomials, DQM, and Herencia *et al's* CF formulation (Eq. 29) for different fibre orientations closely matches the FE results as shown in Fig. 2. The mode shape of the $[+45]_n$ SSSS long plate computed by the RR method is validated by the appropriate FE result shown in Fig. 3. Therefore, the effect of flexural-twist anisotropy is well captured for long anisotropic plates using Herencia *et al* (Herencia et al. 2010) CF expressions with SSSS boundary conditions, given by

$$K_x^{cr} = 2\sqrt{1 - 4\delta\gamma - 3\delta^4 + 2\delta^2\beta} + 2(\beta - 3\delta^2) \tag{29}$$

SSSS square plate

Numerical results of nondimensional buckling coefficients of an SSSS anisotropic square plate for angle-ply laminates computed by FE, DQM, RR and LM methods as well as the H-R principle are listed in Table 1. It is noted that to the authors' best knowledge no CF solutions exist. Error percentages in buckling coefficients for each method when compared with FE results are shown in Table 1. In DQM, the number of grid points was chosen to be $n_x, n_y = 31$ for the analysis. The unidirectional laminates with a ply angle of 45° exhibit high values of both D_{16} and D_{26} flexural-twist anisotropy and causes very slow convergence of the RR method and DQM. DQM overestimates the buckling coefficient by 11.3% for the ply angles 40° ∼ 45° when compared with FE results. The RR method exhibits an approximately 7% error for the ply angles $40° \sim 45°$, even when a relatively large number (23-by-23 terms) of Legendre polynomials were used. The inability of the DQM and RR method to model the effect of flexural-twist anisotropy and the constraints due to boundary conditions are the main reasons for their failure to capture accurate results. As seen from the Table 1, both the approaches based on the LM method and the H-R principle were able to capture the above mentioned constraints and achieved buckling coefficient results with error less than 2.5%. The LM results shown in Table 1 were computed using MN=13 terms for deflection and used 11 Lagrangian multipliers to constrain the geometry boundary conditions along each edge. Fig. 4 demonstrates good convergence of buckling coefficients for the $[+45]_n$ SSSS square plate using the H-R variational principle with only a few polynomial terms in the admissible functions, but does not provide bounded solutions. Fig. 5 shows that the buckling mode shape of the $[+45]_n$ SSSS square plate closely matches FE when only a relatively small number of polynomial terms is used in the series. In this approach, MN (shorthand for M and N) represents the number of terms to represent deflection and moments functions requires more terms than deflection functions for obtaining solutions. The H-R results presented in Table 1 were computed using MN=7 terms for deflection and MN+2 terms for moment functions and the results did not exhibit bounded solution because of the variation of convergence behaviour with ply layups. Therefore, by choosing an appropriate number of polynomials in both approaches, results with good accuracy can be achieved.

SSSF long plate

Numerical results of a long anisotropic plate ($a/b = 20$) with SSSF boundary conditions for all unidirectional layups are presented in this section. The FE results (Fig. 6) show that two possible buckling mode shapes exists and so confirms preliminary results (Weaver and Herencia 2007). The first mode shape is asymmetrical, largely skewed to one side of the plate and the alternative mode shape is nearly symmetrical in nature. For the laminates with ply angle less than 45°, the D_{16} bending-twist anisotropy is high and the plate exhibits a shear instability near the boundary resulting in twisting of the free edge to one side of the plate. But, for laminates with layup greater than 45°, the D_{16} bending-twist anisotropy is relatively low and the plate exhibits almost symmetrical bending behavior of the free edge similar to orthotropic plates. Weaver and Herencia (Weaver and Herencia 2007) proposed one-term expressions to approximately represent each mode shape in Fig. 6. By assuming the mode shape with one side skewed to be $w = w_0 e^{-qx/a} sin(m\pi x/a)y$ and the second mode shape as $w = w_0 sin(m\pi x/a - ky)y$, the following CF solutions of buckling coefficient were derived and are given by,

$$\begin{aligned} K_x^{cr} &= 12\epsilon - \frac{36}{5}\gamma^2 \quad \text{(CF1)} \\ K_x^{cr} &= 12\epsilon - 12\delta^2 \quad \text{(CF2)} \end{aligned} \tag{30}$$

where $\epsilon = D_{66}/\sqrt{D_{11}D_{22}}$. Further insight into these two mode shapes can be obtained as follows. By considering the zero moment boundary condition and $\kappa_y = 0$ along the short edge where the mode shape is skewed, the following relations along this boundary are obtained, as

$$\begin{aligned} M_x =& D_{11}\kappa_x + D_{12}\kappa_y + D_{16}\kappa_{xy} = 0 \Rightarrow \\ \kappa_x =& -\frac{D_{16}}{D_{11}}\kappa_{xy} \Rightarrow \\ M_{xy} =& D_{16}\kappa_x + D_{26}\kappa_y + D_{66}\kappa_{xy} = (D_{66} - \frac{D_{16}^2}{D_{11}})\kappa_{xy} \end{aligned} \tag{31}$$

where $\kappa_x, \kappa_y, \kappa_{xy}$ are bending curvatures of plate. Such analysis shows that the effective twisting stiffness, D_{66} is reduced by the presence of D_{16}. Examining the form of CF1 shows the same functional dependence on D_{66}, D_{11} and D_{16} but the effective twisting stiffness defined in Eq. (31) is less than that given by CF1. A similar formula to CF1 is obtained directly from the orthotropic buckling formula (Weaver and Herencia 2007) but substituting the reduced torsional stiffness from Eq. (31) for D_{66}. Examining the skewed mode shape in Fig. 6 shows the shear instability is in the proximity of the short edge where both M_x and κ_y are close to zero. However, the maximum buckling amplitude is a short distance from the edge where these conditions are no longer exactly satisfied and the effective torsional stiffness would be expected to be larger than the lower bound value given by Eq. (31). As such, it is expected that the true buckling load to lie between CF1 and the lower bound value using Eq. (31) for the torsional stiffness. Thus, CF1 in Eq. 30 is modified to

$$K_x^{cr} = [12\epsilon - 12\gamma^2] \quad \text{(CF-lowerbound)} \tag{32}$$

which usurps, and improves upon, the empirical CF formula given in Weaver and Herencia 2007. Furthermore, an analogous argument along the long, simply supported edge (M_y and $\kappa_x = 0$) provides a torsional stiffness reduced by the presence of D_{26}. In fact, if this reduced torsional stiffness is substituted for D_{66} then one obtains CF2 directly.

The numerical results computed using the RR method, Weaver's CF expressions (Weaver and Herencia 2007), DQM and FE analysis are shown in Fig. 7. For ply angles larger than 45°, Weaver's CF solutions, RR and DQM results matches well with the FE results. However, when ply angles are in the range of

$10^\circ \sim 40^\circ$, the results of all the methods show large inaccuracy compared with FE. For the case of $[+30]_n$, the RR method used 23 by 23 terms of Legendre polynomials in the admissible functions and the error was found to be in excess of 25% when compared with FE results. Using more Legendre polynomial terms is beyond the precision of our current computer capacity and leads to numerical ill-conditioning problems.

For laminates with ply angles larger than 40°, the buckling mode shape evaluated by all of the methods were found to be similar to the second mode shape shown in Fig. 6 and the buckling coefficients matched the FE results. For laminates with ply angle less than 40°, the first buckling mode shape as shown in Fig. 6 was found to be skewed to one side of the plate and the RR method was not able to capture the mode shape accurately resulting in non-physical high buckling coefficient values, as shown in Fig.7. In addition, there were difficulties in representing the mode shape analytically in this angle range and the critical buckling loads computed using analytical methods become very sensitive to the assumption of mode shape functions. Buckling analysis carried out by DQM could only capture the second symmetric mode shape and resulted in over estimation of buckling load. The above results indicate that a robust numerical methodology has to developed to solve the buckling load solutions of laminated plates with strong flexural-twist anisotropy.

To this end, the extreme case of $[+30]_n$ SSSF long plate ($a/b = 20$) was analysed in detail using the Lagrangian multiplier approach. The number of Lagrangian multipliers along the edges in Eq. (12) were chosen to be $2 - 6$ less than the number of terms used in admissible functions (P=Q=PQ, M=N=MN, PQ=MN$-2\ldots-6$). When all the boundary conditions in Eq. (14) were fully satisfied by using Lagrangian multipliers, the plate becomes stiffer and gives an upper bound solution. When the number of Lagrangian multipliers is reduced, constraints on the plate, along the edges, are relaxed and it results in a lower estimation of buckling load. Fig. 8 illustrate the convergence trend of buckling coefficients (K_x^{cr}) by varying the number of Lagrangian multipliers. The upper and lower bounds of K_x^{cr} of $[+30]_n$ SSSF long plate are found in Fig. 8, for this case an exact solution is not possible and the RR method suffers very slow convergence. It can be seen that the FE result falls within the obtained bounds computed by this approach and can be used to confirm accurate buckling load results.

In the H-R variational principle approach, the accuracy and convergence of the buckling load results are studied for the $[+30]_n$ SSSF long plate ($a/b = 20$) by varying the number of terms of Legendre polynomials to represent deflection and moments. Fig. 9 demonstrates good convergence of the buckling coefficients towards FE results using this approach. The mode shape as shown in Fig. 10 was computed using few polynomial terms (5 or 10) for the deflection function and closely matches the FE solution. Hence, the above approach gives valuable insight in to the number of terms in deflection and moment functions to get better results. By using more terms to represent the moment functions than the deflection function makes the plate stiffer and always results in upper bound solution to the FE result.

Figs. 8 and 9 shows that the accuracy of buckling solutions when compared with FE results is affected by the chosen number of Lagrangian multipliers and the number of terms used in moment functions. Hence, appropriately choosing the number of these terms is important for the robustness of both proposed approaches. The optimal number can be selected based on that which gives good convergence (i.e. upper or lower bound). The proposed approaches works well for plates with low flexural anisotropy and exhibits convergence similar to the RR approach. For the case of laminated plates with extremely high flexural anisotropy studied in this paper, the proposed approaches can be used as benchmarks to choose the number of Legendre polynomials for representing deflection functions, moment functions and Lagrangian multipliers. The chosen number of terms varies with different plate boundary conditions. For the buckling problem of SSSF long plate: (i) 21 terms of Legendre polynomials for the deflection function (MN) and 17 Lagrangian multipliers (PQ) along each edge were chosen in the LM method; (ii) in the H-R principle, 10 terms for deflection function and 13 terms for each moment function ($M_iN_i = 13$) were used. These selections were based on the results presented in Figs. 8 and 9 for the $[+30]_n$ SSSF long plate. Both the LM method and the H-R principle were then applied to all the angle orientations of the SSSF long plate ($[+\theta]_s$) and the results are shown in Fig. 11. The buckling load solutions obtained using these two approaches closely match the FE solutions for all the angle-ply orientations. The results obtained using the H-R variational principle were closer to the FE result than the LM approach.

CONCLUSION

The buckling problems of anisotropic plates with strong flexural-twist coupling under different boundary conditions have been investigated. The drawbacks of both DQM and the RR method to accurately model constraints due to high flexural-twist anisotropy for some specific cases ($[+45]_n$ SSSS square plate and $[+30]_n$ SSSF long plate) were discussed. In these cases, the distorted buckling mode shapes were difficult to represent analytically (due to localised deformations) and the CF solutions were unable to predict correct buckling load results. In order to model these problems accurately, two numerical methodologies based on the Lagrangian mulitplier concept and Hellinger-Reissner variational principle were proposed. In the LM approach, the orthogonality of the admissible functions and satisfaction of essential boundary conditions along the edges were ensured by selecting appropriate Lagrangian multiplier terms. The most important advantage of this approach was its ability to provide the upper and lower bounds of buckling coefficient. This approach also ensured fast convergence of buckling load solution by using few polynomials when compared to the RR method.

In the approach based on the Hellinger-Reissner variational principle, both the essential and natural boundary conditions were captured effectively. The most distinct advantage of using this approach is that it can obtain accurate results with very limited number of terms in the admissible functions when compared to other approaches. On the other hand, the variational principle also has some issues for the buckling analysis of composite plates. For example, it can generate different levels of convergence when choosing different numbers of terms in the admissible functions, which makes them difficult to identify converged results. The efficiency will be significantly decreased with an increase of number of terms, as it requires a significantly larger matrix (to invert) than the RR method. However, the mixed variational approach provides insight in to the study of flexural-twist anisotropy on buckling solutions.

Finally, a closed form formula has been offered as a lower bound estimate of buckling load of a long, simply supported, flexurally anisotropic plate, with one long edge free.

REFERENCES

Ashton, J. (1969). "Analysis of anisotropic plates 2." *Journal of Composite Materials*, 3(3), 470–479.

Ashton, J. and Waddoups, M. (1969). "Analysis of anisotropic plates." *Journal of Composite Materials*, 3(1), 148–165.

Balabuch, L. (1937). "The stability of plywood plates." *Aeronautical Engineering, USSR*, 11.

Bellman, R.E. & Casti, J. (1971). “Differential quadrature and long-term integration.” *J Math Anal Appl*, Vol. 34, 235?.

Bhat, R. (1985). “Natural frequencies of rectangular plates using characteristic orthogonal polynomials in Rayleigh-Ritz method..” *Journal of Sound and Vibration*, 102(4), 493 – 499.

Budiansky, B. and Hu, P. C. (1946). “The lagrangian multiplier method of finding upper and lower limits to critical stresses of clamped plates.” *NACA,*, Report No. 848.

Chamis, C. C. (1969). “Buckling of anisotropic composite plates.” *J. Struct. Div.*, 95(ST10), 2119?139.

Chien, W.-Z. (1984). “Generalized variational principles in elasticity.” *Engineering Mechanics in Civil Engineering*, 29, 93–153.

Chow, S., Liew, K., and Lam, K. (1992). “Transverse vibration of symmetrically laminated rectangular composite plates.” *Composite Structures*, 20(4), 213–226.

Darvizeh, M., Darvizeh, A., Ansari, R., and Sharma, C. B. (2004). “Buckling analysis of generally laminated composite plates (generalized differential quadrature rules versus RayleighRitz method).” *Composites and structures*, Vol. 63, 69–74.

Green, A. and Hearmon, R. (1945). “The buckling of flat rectangular plywood plates.” *Philosophical Magazine*, 7, 659–688.

Grenestedt, J. L. (1989). “Study on the effect of bending-twisting coupling on buckling strength.” *Composite Structures*, 12(4), 271 – 290.

Herencia, J. E., Weaver, P. M., and Friswell, M. I. (2010). “Closed-form solutions for buckling of long anisotropic plates with various boundary conditions under axial compression.” *Journal of Engineering Mechanics*, 136(9), 1105–1114.

Liew, K. and Wang, C. (1995). “Elastic buckling of regular polygonal plates.”

Thin-Walled Structures, 21(2), 163–173.

Nemeth, M. P. (1986). “Importance of anisotropy on buckling of compression-loaded symmetric composite plates.” *AIAA journal*, 24(11), 1831–1835.

Pandey, M. D. and Sherbourne, A. N. (1991). “Buckling of anisotropic composite plates under stress gradient.” *Journal of Engineering Mechanics*, 117(2), 260 – 275.

Plass, H. J., Gaines, J. H., and Newsom, C. D. (1962). “Application of reissner’s variational principle to cantilever plate deflection and vibration problems.” *Journal of Applied Mechanics*, 29, 127–135.

Reissner, E. (1950). “On a variational theorem in elasticity.” *Journal of Mathematics and Physics*, 29(2), 90–95.

Sherbourne, A. N. and Pandey, M. D. (1991). “Differential quadrature method in the buckling analysis of beams and composite plates.” *Computers and Structures*, 40, 903–13.

Shu, C. (2000). *Differential quadrature and its application in engineering*. London: Springer-Verlag.

Smith, S. T., Bradford, M. A., and Oehlers, D. J. (1999). “Numerical convergence of simple and orthogonal polynomials for the unilateral plate buckling problem using the RayleighRitz method.” *International Journal for Numerical Methods in Engineering*, 44(11), 1685–1707.

Tang, W.-Y. and Sridharan, S. (1990). “Buckling analysis of anisotropic plates using perturbation technique.” *Journal of Engineering Mechanics*, 116(10), 2223 – 2236.

Thielemann, W. (1950). “Contribution to the problem of buckling of orthotropic plates, with special reference to plywood.” *NACA Technical Memorandum 1263*.

Washizu, K. (1975). *Variational Methods in Elasticity and Plasticity, second edi-*

tion. Pergamon Press, London.

Weaver, P. M. (2006). "Approximate analysis for buckling of compression loaded long rectangular plates with flexural/twist anisotropy." *Proceedings of the Royal Society A: Mathematical, Physical and Engineering Science*, 462(2065), 59–73.

Weaver, P. M. and Herencia, J. E. (2007). "Buckling of a flexurally anisotropic plate with one edge free." *AIAA/ASME/ASCE/AHS/ASC Structures, Structural Dynamics and Materials Conference*, 8, 8534 – 8542.

Weaver, P. M. and Nemeth, M. P. (2007). "Bounds on flexural properties and buckling response for symmetrically laminated composite plates." *Journal of Engineering Mechanics*, 133(11), 1178 – 1191.

Whitney, J. (1972). "Free vibration of anisotropic rectangular plates." *Journal of the Acoustical Society of America*, 52(1 Part 2), 448 – 449.

TABLE 1. Buckling Coefficient K_x^{cr} of $[+\theta]_n$ SSSS square plate

θ	FE	DQM	RR (MN=23)	LM (MN=13)$^{\dagger 1}$	H-R (MN=7)$^{\ddagger 2}$
0	9.240	9.240 (0.00)	9.240 (0.00)	9.240 (0.00)	9.240 (0.00)
10	8.311	8.401 (1.08)	8.407 (1.15)	8.393 (0.98)	8.404 (1.11)
20	5.332	5.379 (0.87)	5.413 (1.51)	5.364 (0.59)	5.385 (0.99)
30	2.923	3.063 (4.82)	3.026 (3.52)	2.906 (0.59)	2.919 (0.12)
40	1.997	2.223 (11.3)	2.144 (7.36)	1.948 (2.44)	1.959 (1.91)
45	1.839	2.043 (11.1)	1.968 (7.03)	1.795 (2.40)	1.804 (1.87)
50	1.807	1.880 (4.03)	1.856 (2.71)	1.771 (1.96)	1.780 (1.49)
60	1.819	1.884 (3.58)	1.881 (3.41)	1.812 (0.40)	1.830 (0.60)
70	2.303	2.286 (0.76)	2.339 (1.56)	2.311 (0.33)	2.337 (1.45)
80	2.638	2.661 (0.88)	2.664 (1.02)	2.655 (0.68)	2.666 (1.06)
90	2.545	2.561 (0.61)	2.561 (0.61)	2.561 (0.61)	2.561 (0.62)

[1] † 11 Lagrangian multipliers were used for boundary conditions along each edge.

[2] ‡ 9 terms were used for each moment function.

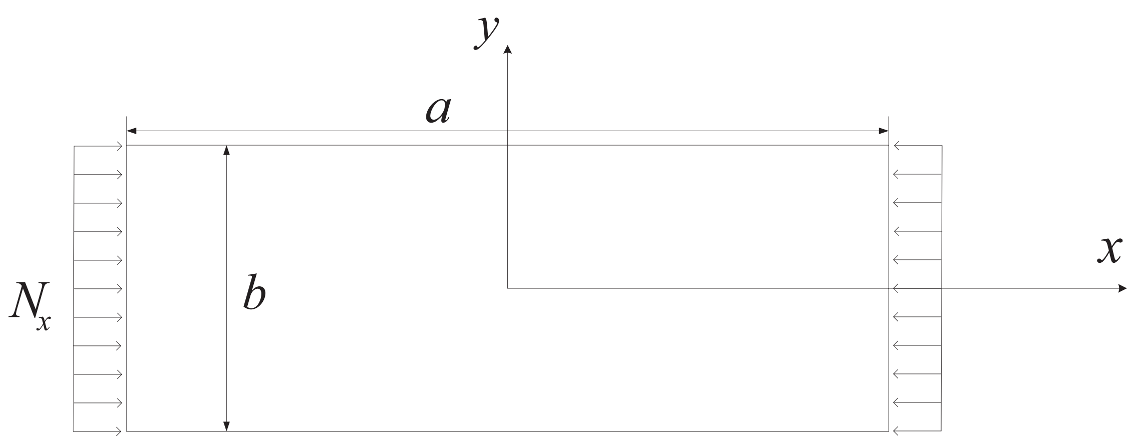

FIG. 1. Load and geometry of anisotropic plates

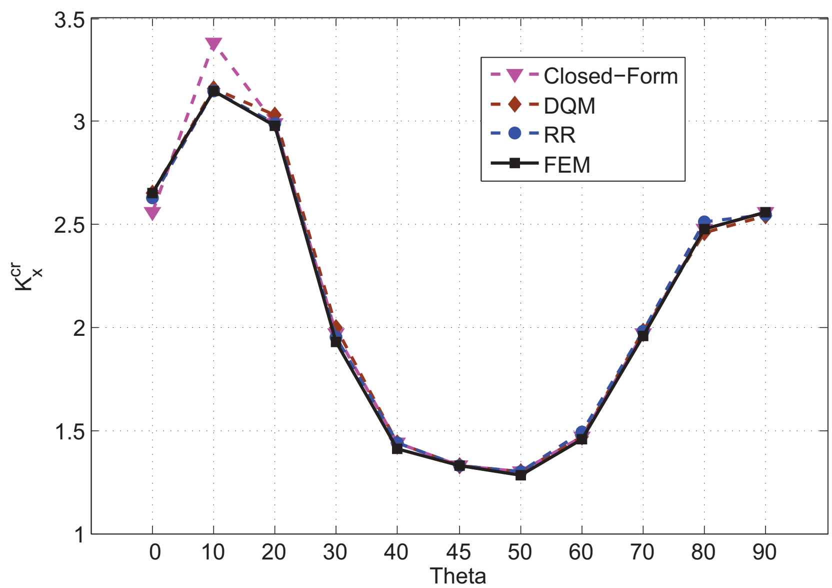

FIG. 2. Buckling coefficients vs. ply angles for $[+\theta]_n$ SSSS long plate ($a/b = 5$).

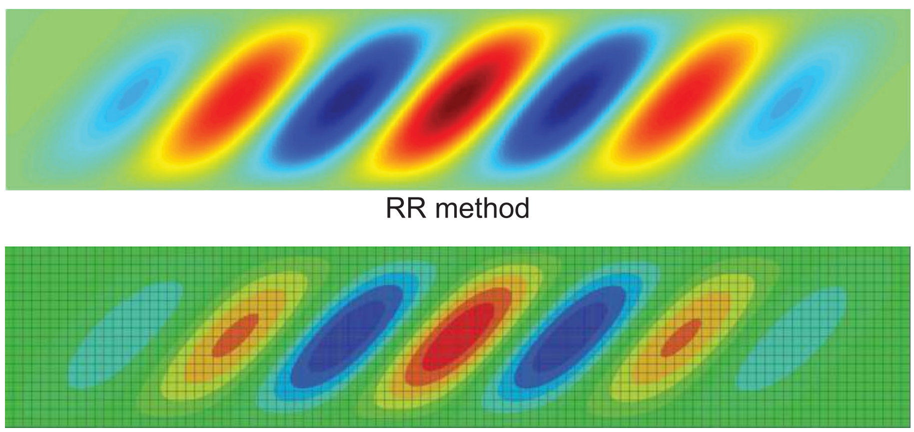

FIG. 3. Buckling mode shapes of $[+45]_n$ SSSS long plate ($a/b = 5$) obtained by RR method and FE.

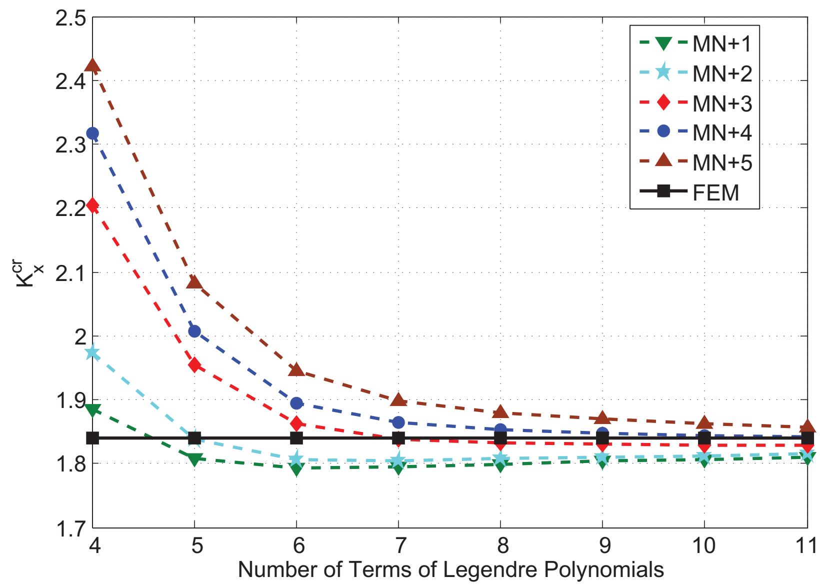

FIG. 4. The convergence trend of non-dimensional buckling coefficient (K_x^{cr}) of $[+45]_n$ SSSS square plate varying with the number of terms (M, N) in admissible functions using the H-R principle. Different curves in this plot represent different number of terms used in the moment functions where MN represents the number of terms in the deflection function.

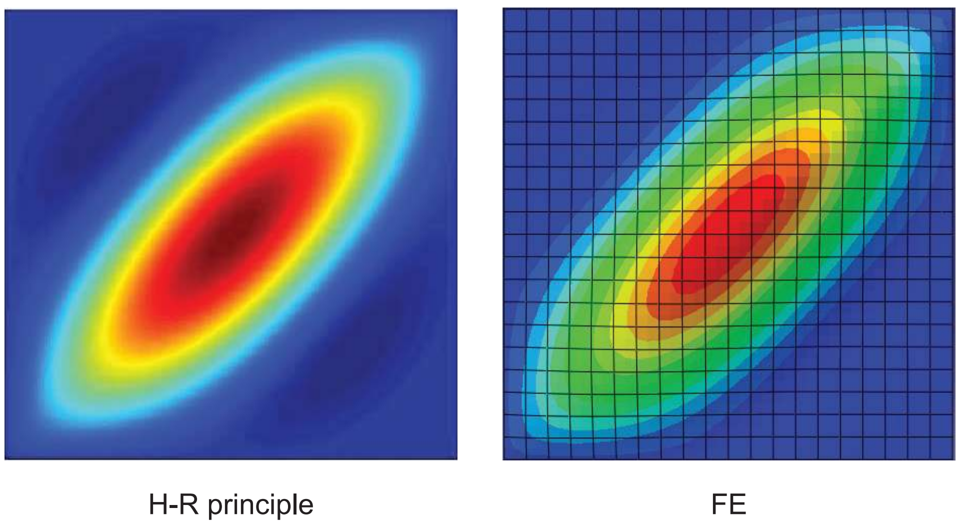

FIG. 5. Buckling mode shapes of $[+45]_n$ SSSS square plate obtained by using H-R principle and FE.

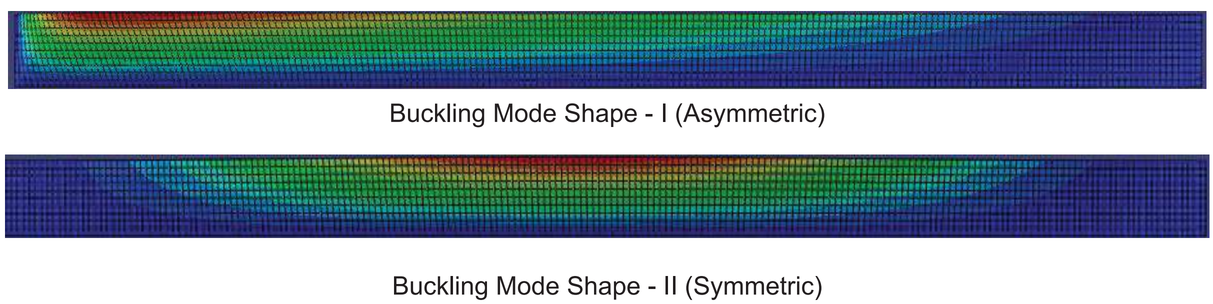

FIG. 6. Buckling mode shapes of $[+\theta]_n$ SSSF long plate (FE).

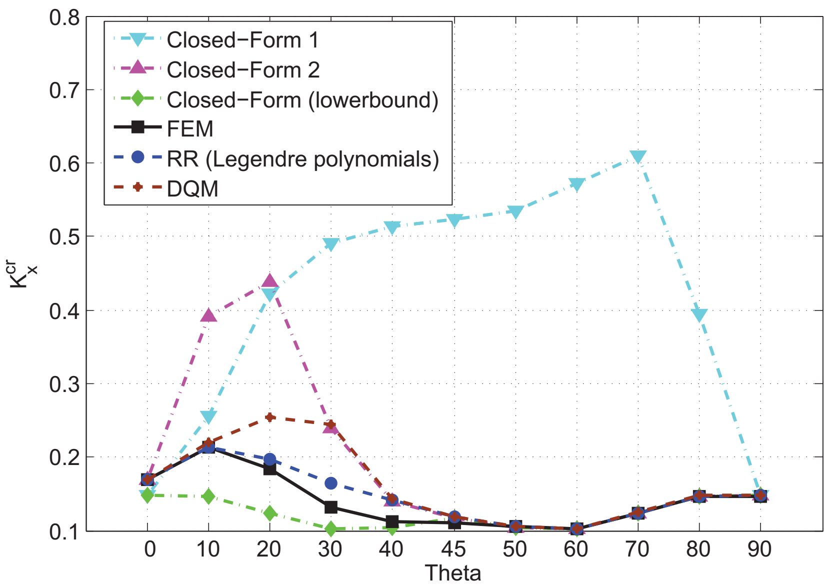

FIG. 7. Buckling coefficients vs. ply angles for $[+\theta]_n$ SSSF long plate.

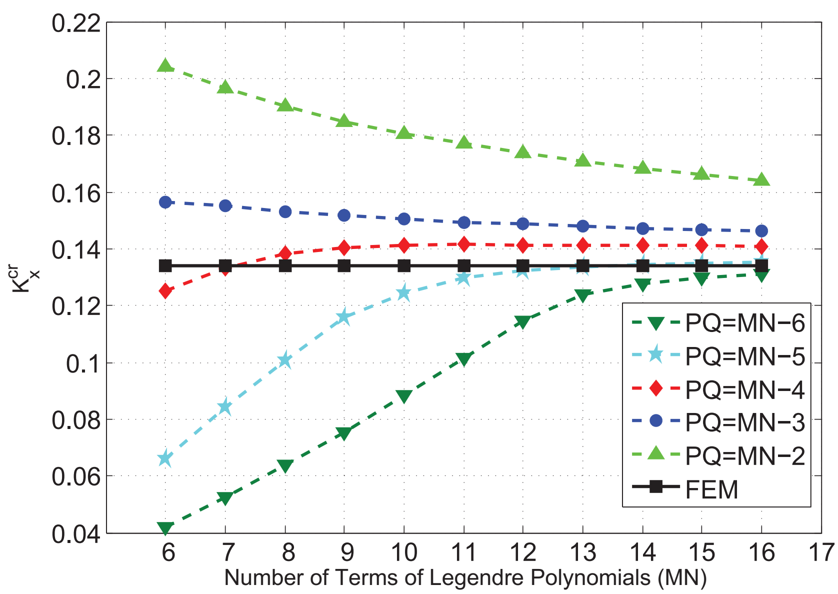

FIG. 8. The convergence trend of the non-dimensional buckling coefficient (K_x^{cr}) of $[+30]_n$ SSSF long plate ($a/b = 20$) varying with the number of terms (M, N) in admissible functions using the LM method. Different curves in this plot represent different number of Lagrangian multipliers.

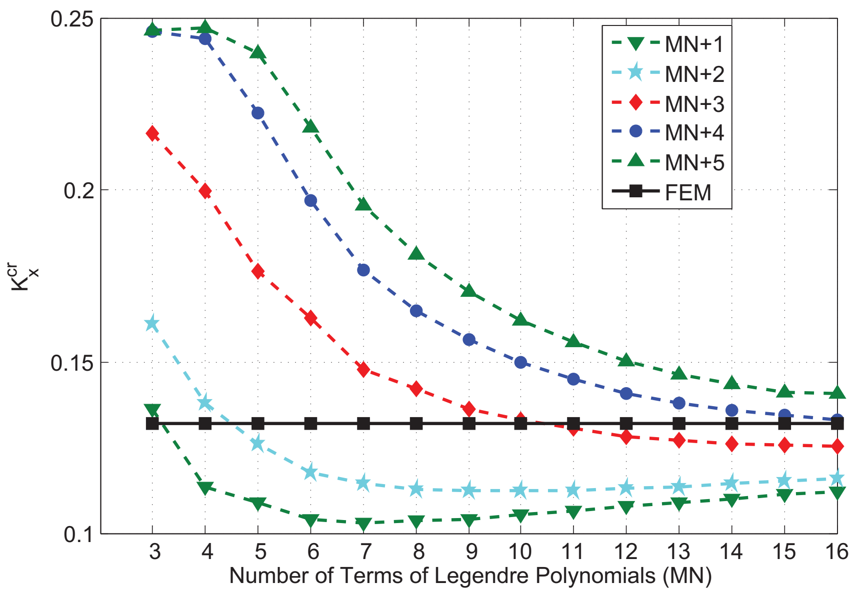

FIG. 9. The convergence trend of non-dimensional buckling coefficient (K_x^{cr}) of $[+30]_n$ SSSF long plate ($a/b = 20$) varying with the number of terms (M, N) in admissible functions using the H-R principle. Different curves in this plot represent different number of terms used in the moment functions where MN represents the number of terms in the deflection function.

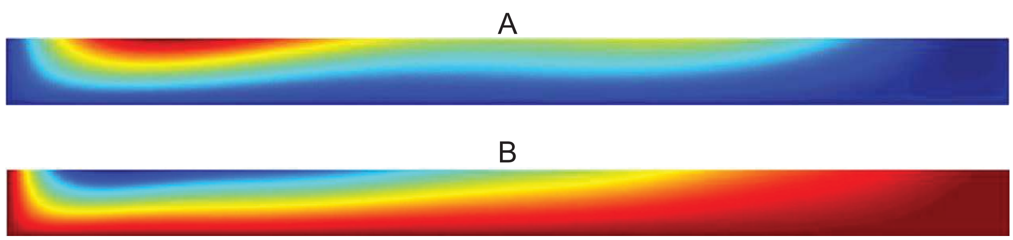

FIG. 10. The buckling mode shapes obtained using the H-R principle with different number of terms of Legendre polynomials of the admissible functions. (A)5 terms for each deflection function and 8 terms for each moment function. (B)10 terms for the deflection and 14 terms for each moment function.

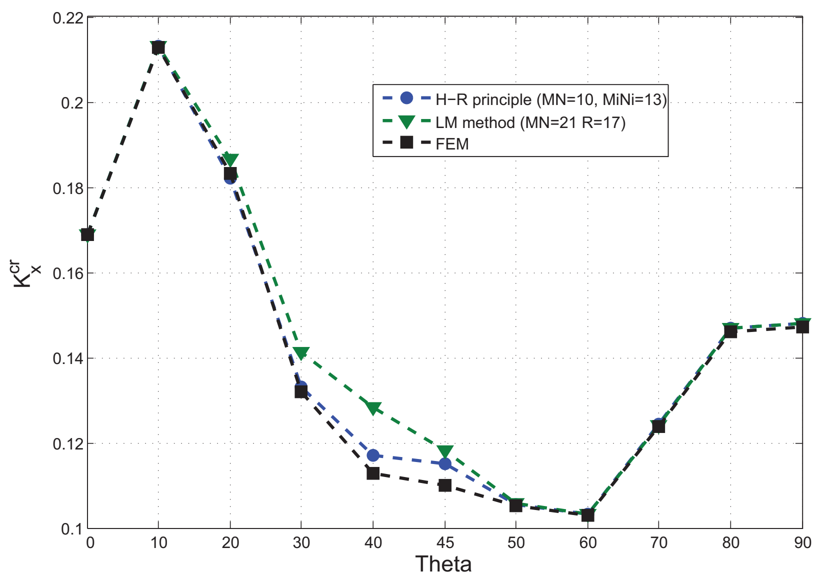

FIG. 11. Non-dimensional buckling coefficients varying with fibre angle for $[+\theta]_n$ SSSF long plate obtained by using the LM method and the H-R principle.